PRIMA

Small or medium-scale focused research project

SEVENTH FRAMEWORK PROGRAMME

THEME FP7-ICT-2009-4

INFORMATION SOCIETY TECHNOLOGIES

Deliverable 2.3 – Define optimal solution-based metal NPs (solvent, capping layer, size, shape) for near vs. far-field effects

Contract no.:	248154
Project acronym:	PRIMA
Project full title:	Plasmon Resonance for IMproving the Absorption of solar cells
Project website:	http://www.prima-ict.eu

Coordinator contact details: Barry P. Rand (rand@imec.be)
IMEC
Kapeldreef 75
B-3001 Heverlee
Belgium
Tel: +32-16-287780
Fax:+32-16-281097

Document revision history

Version	Date	Author	Summary of main changes
1	30.08.2011	Bjoern Niesen	Particles in organic solar cells
2	31.08.2011	Pol Van Dorpe	Particles on silicon solar cells.

Table of Contents:

1 Solution processed silver nanoparticles for silicon solar cells

For silicon solar cells we are mainly focusing on scattering approaches and therefore we investigated relatively large Ag nanoparticles close to the front-side of the silicon substrate. Different spacer thicknesses and capping layers are investigated.

1.1 Nanoparticle synthesis and characterization

Ag nanoparticles were synthesized and deposited on a glass reference wafer and a Si solar cell as explained below:
Materials

Commercial silver nanoparticles coated with Polyvinylpyrrolidon (PVP) were bought from Blue Nano (China). The nanoparticles show a large polydispersity (a polydispersity index of 0.4 as measured by Dynamic Light Scattering; Zetasizer NanoZS, Malvren instruments). These particles were used as such in a first experiment, but in a later experiment, filtered to obtain a more uniform size distribution. Therefore, the nanoparticles were centrifuged for 10 min at a speed of 7500 rpm (rotor radius 99.83 mm). The supernatant, containing small AgNP, was kept separately. This small fraction of AgNPs was centrifuged two times more to get rid of the bigger nanoparticles. The final solution contained a homogeneous nanoparticle suspension with an average size of 274 +/- 6 nm (PDI of 0.1).

The samples (quartz or silicon) were cleaned with a piranha solution for 10 min. A solution of 95:5 ethanol /H_2O was prepared containing 10% 3-mercaptopropylmethoxysilane (Sigma Aldrich). Immediately after rinsing the fresh cleaned samples with H_2O, they were immerged in the silane solution and incubated at room temperature for 3 hours. Then the samples were baked for 10 min in an oven at 110°C. Finally these silanised samples were immerged in the AgNP suspension and incubated overnight to obtain silver-coated samples.

Fig. 1 shows the deposited Ag nanoparticles and their optical extinction spectrum (on glass).

(a) 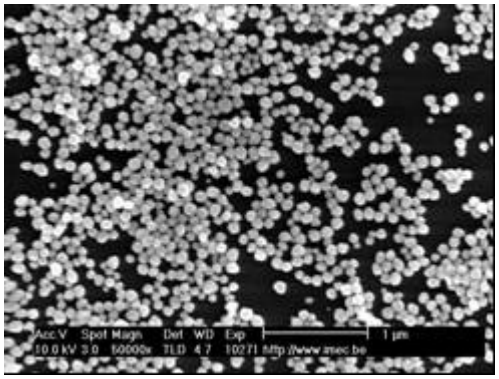

(b) 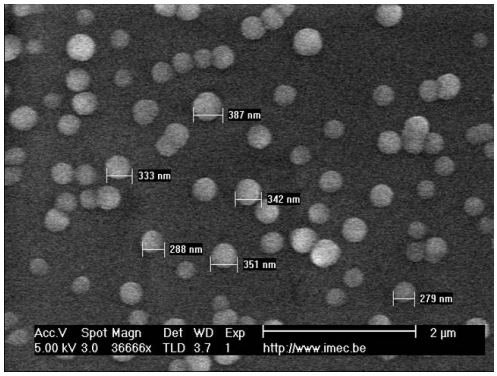

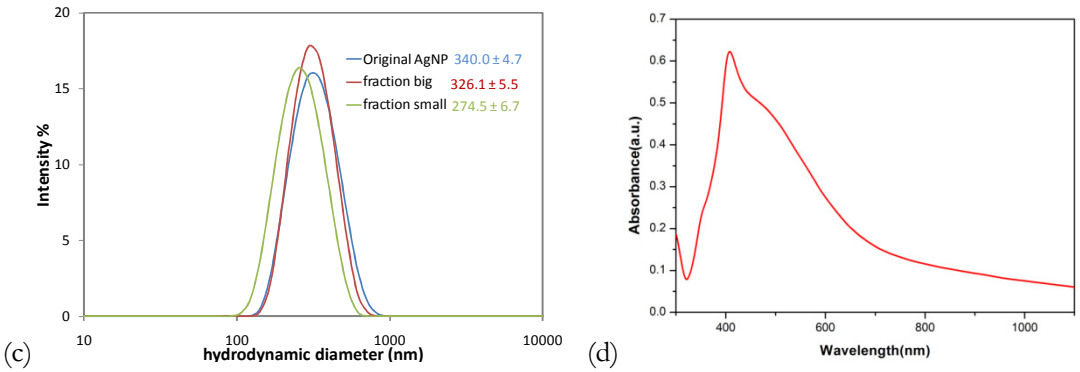

(c) (d)

Fig. 1 (a) SEM image of the Ag nanoparticles. (b) zoom-in of the particles, showing diameters of ~270 to 350 nm (c) a measurement of the size distribution of the particles in suspension using dynamic light scattering before and after size separation. (d) a UV-Vis extinction spectrum of the particles immobilized on a quartz carrier.

The size of the nanoparticles is relatively large and is chosen to act as efficient scatterers. For this size of particles, most of the light impinging on the particles will be scattered instead of absorbed. The extinction spectrum as shown in Fig. 1(d) shows actually that the resonance consists of a small octupolar peak (<400 nm), a large quadrupolar peak (~400 nm) and a broader dipolar peak at around 500 nm. We expect that the different multipoles will have a different scattering behaviour and hence a different effect on the solar cell optical response.

1.2 Optical properties of nanoparticles on silicon

The Ag nanoparticles were deposited on top of a poly-crystalline non-processed Si solar cell fabricated using Al-induced crystallization using the above described mercapto-silanization procedure. The particles are deposited either directly on the Si (still covered with the native oxide) or on a thin SiO_2 spacer layer. After particle deposition, the particles are optionally capped by a SiO_2 layer.

In a first experiment, the particles were deposited on a Si solar cell without spacer layer and capped by a 50 nm oxide coating. The deposition process resulted in a rather inhomogeneous particle distribution, with two different zones: a relatively dense zone – with ~ 5 particles/μm^2 (noted as "dark" zone, due to the clear colour difference) and a less dense zone with ~ 2 to 3 particles/μm^2 (clear zone). This is shown below in two SEM images (Fig. 2)

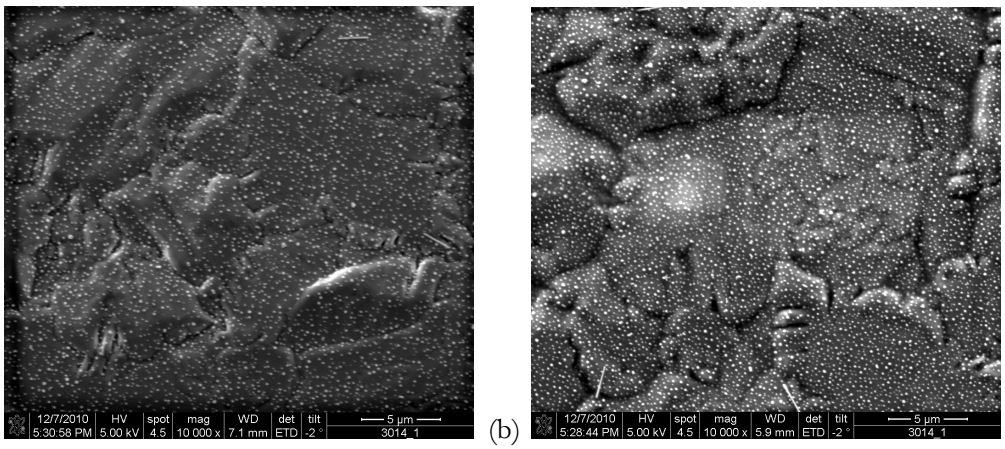

(a) (b)

Fig 2. Particles on poly-crystalline silicon surface of which the grains are visible. The white dots are spherical particles covered with a silicon oxide layer. The two SEM -pictures are representing a different area of the solar cell. There is a difference in density of the particles: (a) 2-3 particles and (b) 5 particles per $\mu m2$.

Both reflection and transmission through the samples was measured using an integrating sphere setup, allowing to measure the sum of specular and diffusion reflection/transmission (R/T). This results in a full optical analysis as the optical absorption can simply be calculated as A=1-R-T. The optical properties were compared with silicon samples without particles and with a 50 nm oxide layer (similar as the capping layer on the particles) and samples withouth particles and with a 100 nm oxide anti-reflective coating layer.

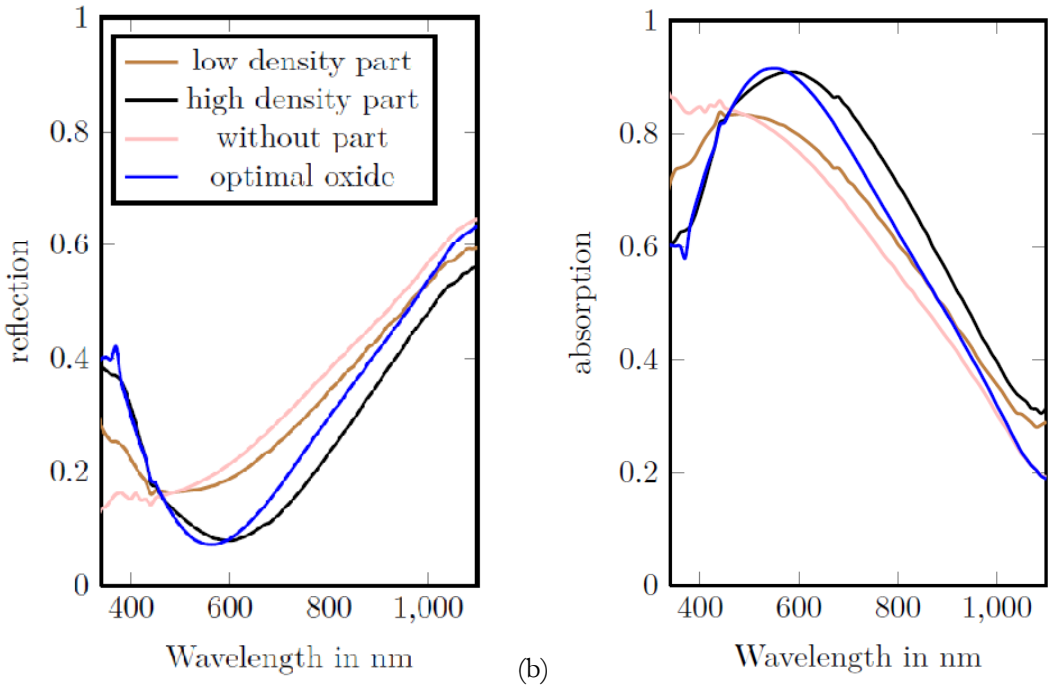

Fig. 3 Reflection (a) and absorption(b) of the samples with and without particles, with high and low density. For a sample with the same oxide thickness (50nm) as on the particles, labeled without part, and for a sample with 100nm of oxide, which is near the optimal thickness that can be formed with silicon oxide.

The results are shown in Fig. 3 and indicate that the dense particle layer shows both much reduced reflection and increased absorption compared to the situation without particles, for wavelengths above 450 nm. Comparing to the sample with anti-reflective coating yields similar results at short wavelength, but increased absorption at longer wavelengths. Still, the resulting reflectance spectra are rather broad and do not clearly show evidence for plasmonic resonances. This is potentially induced by the large inhomogeneity of the particle sizes, smearing out the resonances.

In a second experiment this has been reproduced, but with particles using a narrow size distribution around 274 nm. Moreover, in this case we compared the situation with and without a 10 nm SiO_2 spacer layer and we varied the oxide capping thickness between 110 and 150 nm. The results are shown in Fig. 4 and Fig. 5. It is clear that there are multiple dips present in the reflectance spectra.

The dips can be attributed to dipolar and quadrupolar resonances in the metal nanoparticles. The excitation of multipoles is facilitated by the large size of the particles, but will lead to larger absorption in the particles at these wavelengths. It is, however, clear that the presence of the particles leads to deeper reflection dips compared to the presence of only an anti-reflective coating. This does not mean that the decreased reflection leads to larger cell efficiencies, as the non-reflected power can also be dissipated in the particles. We also looked at the the effect of the capping thickness and noticed (Fig. 5) a small red-shift of the resonances when changing the capping thickness from 110 to 150 nm.

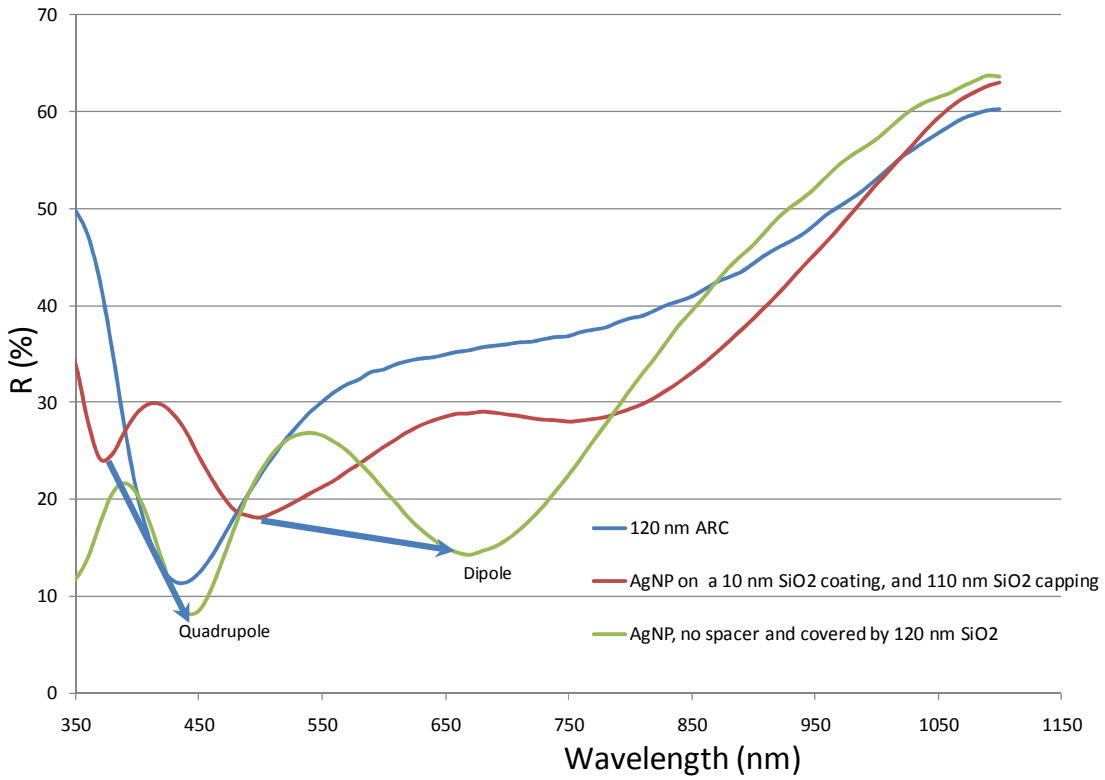

Fig. 4 Reflectance spectra for 274 nm large Ag particles on a Si solar cell with an oxide capping with and without spacer layer between the particles and the oxide. There is a clear red-shift comparing the situation with and without capping. The reflectance dips can hence be attributed to dipole and quadrupole resonances in the particles.

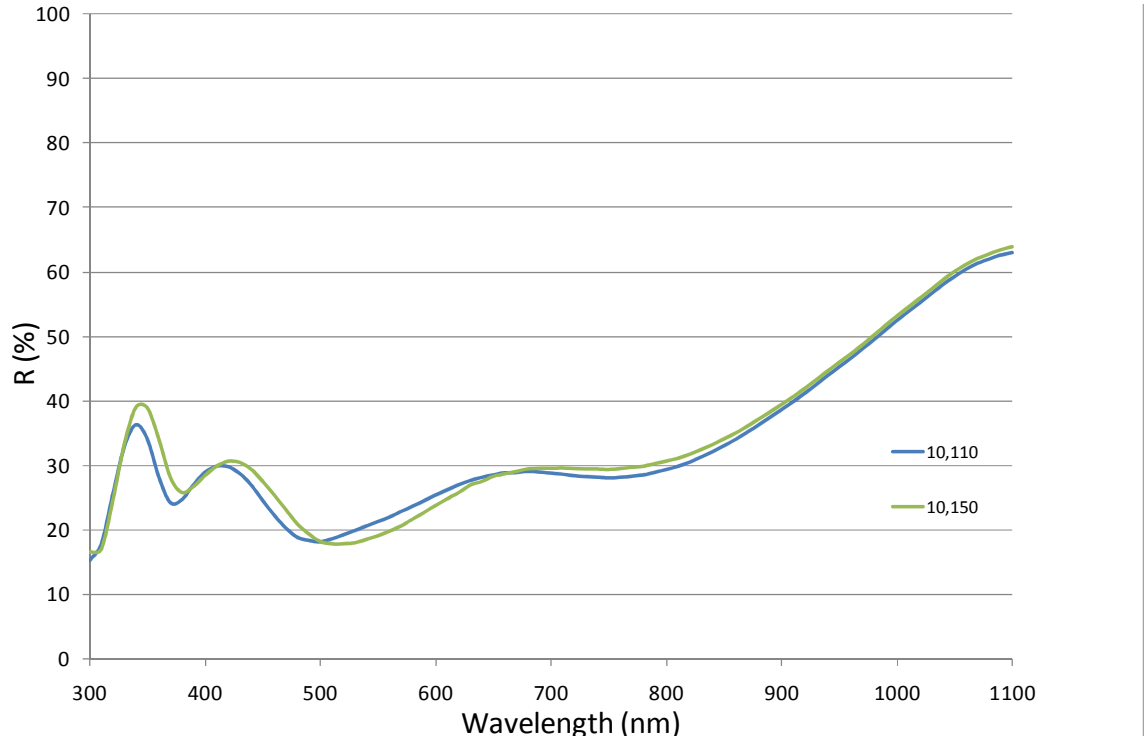

Fig. 5 Reflectance spectra for 274 nm large Ag particles on Si solar cells for different thickness of the oxide capping. Only a small wavelength shift is noticeable.

1.3 Electrical properties of a cell with particles

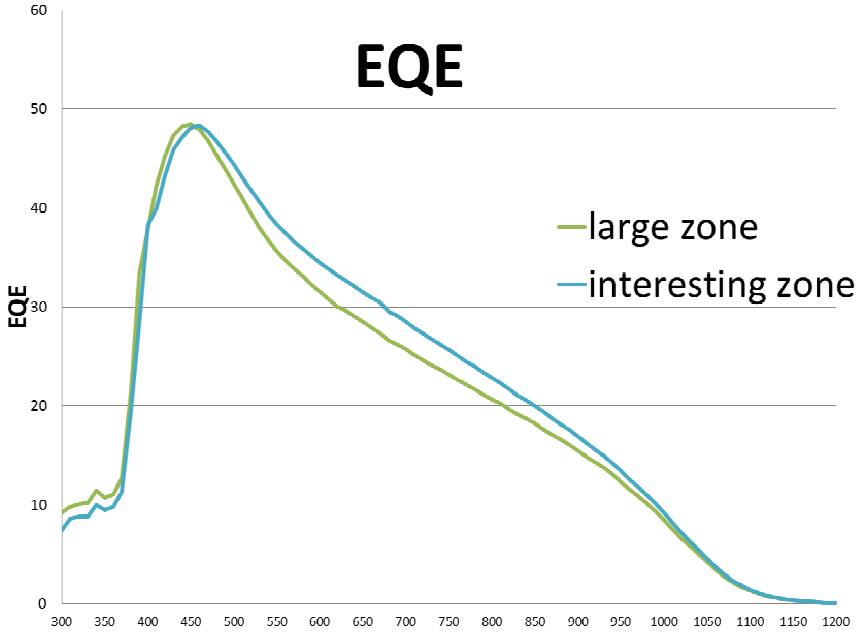

Figure 6 EQE on two zones of the sample, a strong inhomogeneity can be observed.

Obviously, only electrical measurements can show that the enhanced optical absorption is related to a larger creation of electron-hole pairs in the silicon cell. Therefore we finished the cell fabrication of the first run (with the broad distribution of particle sizes) and show the external quantum efficiency (EQE) measurements in Fig. 6. We compare the light zone (large zone) and dark zone (interesting zone, with a higher particle density and consequently smaller reflection). It shows that indeed the EQE is larger for the dense particle zone, especially for the wavelength region between 500 and 900 nm, where the dipolar resonance is expected for particles without oxide spacer. Nevertheless, future tests would require a reference cell for a true performance comparison.

1.4 Conclusion

We have investigated the optical properties of Ag nanoparticles on silicon solar cells and found that for large particles, where the optical response is dominated by scattering, multipole peaks are clearly visible. We have looked into the effect of the nanoparticle capping thickness and have found that this thickness is not critical for the device performance. First EQE tests indicate that indeed performance improvements are possible, but more tests are necessary to give conclusive results.

2 Solution processed gold nanoparticles for organic solar cells

Solution-processed metal nanoparticles for organic solar cells

Embedding metal nanoparticles (NPs) in organic host materials, such as polymers, is not trivial and usually leads to clustering of the particles. In order to reach a homogeneous dispersion, specifically functionalized metal NPs have to be employed. One approach is to coat the nanoparticles with a chemical compound that has a structure

similar to the host material. For this purpose, we synthesized Au NPs that were coated with thiol-functionalized polystyrene chains.

These particles were then given to a solution of MDMO-PPV, a semiconducting polymer, in chloroform and were spin coated to form a thin-film. By means of focused ion-beam transmission electron microscopy, the cross-section of this film was examined [Fig. 1(a)]. As a control experiment, Au NPs coated by the much shorter molecule dodecane-thiol were blended into the polymer layer [Fig. 1(b)]. These micrographs show that the polystyrene capping significantly enhanced the dispersion of the nanoparticles in the polymer host, such that only a fraction of the particles aggregate at the interface compared to the dodecane-thiol capped particles that all aggregate at the interface.

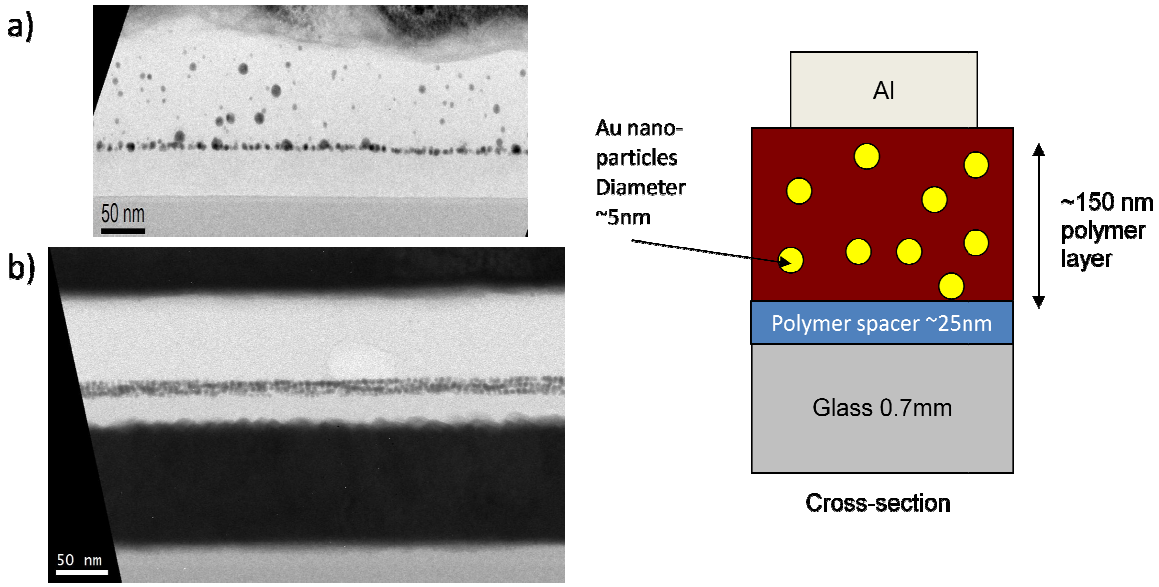

: or (b) dodecane-thiol

After this confirmation of the improved NP dispersion by the polystyrene capping layer, the optical properties of the NPs were characterized (Fig. 2). Both types of NPs show a strong absorption band, which is centered at a wavelength of 510 and 530 nm in the case of the alkanethiol and polystyrene capped NPs, respectively. This absorption band is typical for spherical Au NPs with a diameter much smaller than the wavelength of the incident light and is caused by the excitation of a localized surface plasmon resonance.

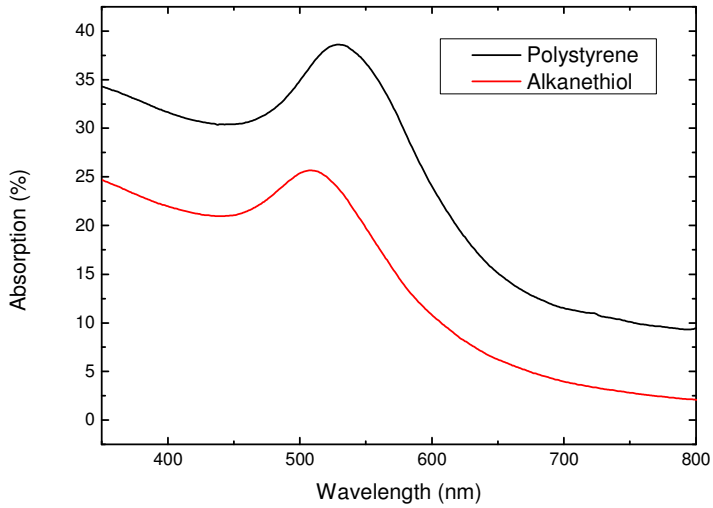

Figure. 2: Absorption spectra of Au NPs capped with either polystyrene or dodecanethiol in solution.

Finally, the impact of these NPs on the electrical properties of organic solar cells was examined. Both types of Au NPs were blended into the active layer of organic solar cells by mixing the solution with the organic semiconductors with the NPs prior to the spin-coating. PEDOT:PSS coated ITO was used as the anode, Yb/Al as cathode. The normalized solar cell efficiency for such solar cells is shown in Fig. 3 versus the NP concentration for both types of capping layers. In both cases, the efficiency strongly decreases with increasing Au NP concentration. Both curves have a similar shape. This indicates that even though a homogeneous dispersion of the NPs in the active layer might be crucial, it is not sufficient to lead to a better solar cell efficiency. Effects such as exciton quenching or charge trapping could dominate any beneficial effect caused by the NPs.

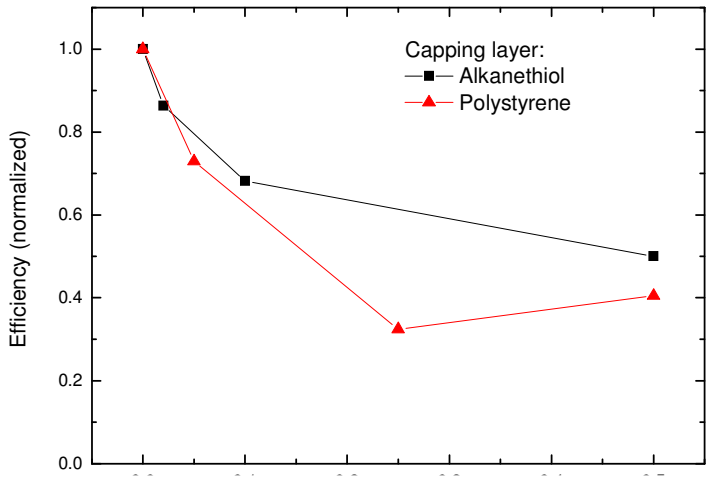

Figure. 3: Normalized efficiency for solar cells containing Au NP capped with either dodecanethiol or polystyrene in the active layer versus the NP concentration.

In
solar cells with either P3HT or MDMO-PPV as electron donor material. The efficiency of both types of solar cells was found to decrease significantly when introducing alkanethiol-capped Au NPs. It decreased from 3.7% to 2.9% for the P3HT cell and from 1.5% to 0.8% in the case of MDMO-PPV. When measuring the external quantum efficiency, the photocurrent was found to decrease over the full absorption spectra of the active layer

materials (Fig. 4). These results suggest that the decrease in efficiency observed when embedding Au NPs in the active layer of organic solar cells is independent of the active layer material.

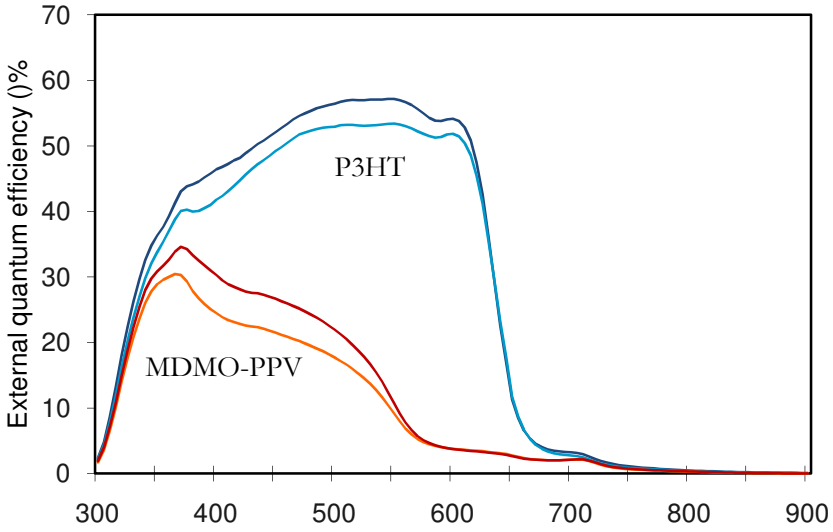

Figure. 4: External quantum efficiency for solar cells with an active layer of P3HT:PCBM or MDMO-PPV:PCBM with (light-colored curves) and without (dark-colored curves) alkanethiol-capped Au NPs